Immunity
Article

Canonical Wnt Signaling Negatively Modulates Regulatory T Cell Function

Jorg van Loosdregt,[1,2,3] Veerle Fleskens,[1,3] Machteld M. Tiemessen,[8] Michal Mokry,[4] Ruben van Boxtel,[3] Jenny Meerding,[2,5] Cornelieke E.G.M. Pals,[1,3] Dorota Kurek,[9] Miranda R.M. Baert,[8] Eveline M. Delemarre,[2,5] Andrea Gröne,[10] Marianne J.A. Groot Koerkamp,[6] Alice J.A.M. Sijts,[11] Edward E.S. Nieuwenhuis,[4] Madelon M. Maurice,[3] Johan H. van Es,[7] Derk ten Berge,[9] Frank C. Holstege,[6] Frank J.T. Staal,[8] Dietmar M.W. Zaiss,[11] Berent J. Prakken,[2,5] and Paul J. Coffer[1,2,3,*]

[1]Department of Immunology
[2]Center for Molecular and Cellular Intervention, Wilhelmina Children's Hospital
[3]Department of Cell Biology
[4]Department of Pediatric Gastroenterology, Wilhelmina Children's Hospital
[5]Department of Pediatric Immunology, Wilhelmina Children's Hospital
[6]Molecular Cancer Research
University Medical Center Utrecht, Utrecht 3584EA, the Netherlands
[7]Hubrecht Institute/KNAW and University Medical Center Utrecht, Uppsalalaan 8, Utrecht 3584CT, the Netherlands
[8]Department of Immunohematology and Blood Transfusion, Leiden University Medical Center, Leiden 2300RC, the Netherlands
[9]Erasmus Stem Cell Institute, Department of Cell Biology, Rotterdam 3015GE, the Netherlands
[10]Department of Pathobiology
[11]Department of Infectious Diseases and Immunology
Faculty Veterinary Medicine Utrecht, Utrecht 3508TD, the Netherlands
*Correspondence: p.j.coffer@umcutrecht.nl
http://dx.doi.org/10.1016/j.immuni.2013.07.019

SUMMARY

Foxp3 is crucial for both the development and function of regulatory T (Treg) cells; however, the posttranslational mechanisms regulating Foxp3 transcriptional output remain poorly defined. Here, we demonstrate that T cell factor 1 (TCF1) and Foxp3 associates in Treg cells and that active Wnt signaling disrupts Foxp3 transcriptional activity. A global chromatin immunoprecipitation sequencing comparison in Treg cells revealed considerable overlap between Foxp3 and Wnt target genes. The activation of Wnt signaling reduced Treg-mediated suppression both in vitro and in vivo, whereas disruption of Wnt signaling in Treg cells enhanced their suppressive capacity. The activation of effector T cells increased Wnt3a production, and Wnt3a levels were found to be greatly increased in mononuclear cells isolated from synovial fluid versus peripheral blood of arthritis patients. We propose a model in which Wnt produced under inflammatory conditions represses Treg cell function, allowing a productive immune response, but, if uncontrolled, could lead to the development of autoimmunity.

INTRODUCTION

Regulatory T (Treg) cells are a specific $CD4^+CD25^+Foxp3^+$ T cell lineage that are crucial for the induction of self-tolerance (Khattri et al., 2003; Fontenot et al., 2003). The Forkhead box transcription factor Foxp3 has been demonstrated to be uniquely required for Treg cell differentiation and function (Khattri et al., 2003; Fontenot et al., 2003). Although $Foxp3^+$ Treg cells are potent suppressors of immune responses, and large numbers of $Foxp3^+$ Treg cells are often found at inflammatory sites in a variety of diseases, including inflammatory bowel disease, type 1 diabetes, multiple sclerosis, systemic lupus, and juvenile idiopathic arthritis (Lindley et al., 2005; Viglietta et al., 2004; Ehrenstein et al., 2004). These findings suggest that, in many autoimmune diseases, Treg cell function may be suppressed by the local inflammatory environment, potentially because of deregulated Foxp3 transcriptional activity.

It has been proposed that the association of Foxp3 with additional transcription factors including NFAT and AML1/Runx1 is essential for Treg-cell-suppressive function (Wu et al., 2006; Ono et al., 2007). Both NFAT and AML1 bind to the promoter of Foxp3 transcriptional targets, including the genes encoding IL-2, CTLA-4, and CD25. Specific mutations in Foxp3 were shown to disrupt the Foxp3-NFAT or Foxp3-AML1 association and impaired Treg-cell-mediated suppression as a result (Wu et al., 2006; Ono et al., 2007).

In an unbiased screen for indentifying modulators of Foxp3 transcriptional activity, we identified the transcription factor T cell factor 1 (TCF1) as a Foxp3 interaction partner. TCF1 is a key transcription factor responding to canonical Wnt signaling and acts as a transcriptional activator in the presence of β-catenin (Staal et al., 2008; Verbeek et al., 1995). β-catenin protein amounts are regulated by a multimolecular destruction complex containing: axis inhibition protein (AXIN), adenomatous polyposis coli, casein kinase 1 (CK1), and glycogen synthase kinase 3β (GSK3β). In the absence of Wnt signaling, β-catenin is phosphorylated by CK1 and GSK3β, subsequently resulting in the polyubiquitination and degradation of β-catenin by the 26S proteasome. The interaction of Wnt with frizzled (FZD) receptor results in the inhibition of GSK3 activity, inactivating the

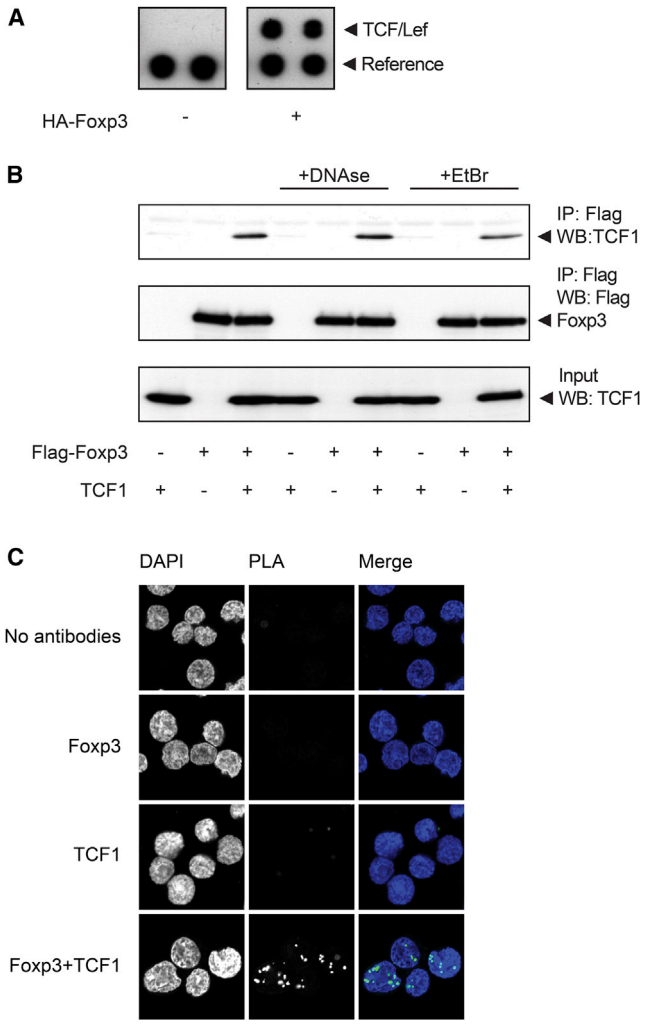

Figure 1. TCF1 Associates with Foxp3 in Human Treg Cells

(A) HA-Foxp3 was immunoprecipitated from HA-Foxp3-transfected HEK 293T cell lysate. Specific biotin-labeled transcription factor binding sites were added, washed, boiled, and hybridized on the TF-TF interaction array. Bound oligos were visualized with streptavidin antibodies.

(B) HEK 293T cells were cotransfected with FLAG-Foxp3 and TCF1. Lysates were treated with 100 U/ml DNase or 25 μg/ml EtBr for 20 min, Foxp3 was immunoprecipitated, and immunoblots were analyzed with antibodies against TCF1 or HA.

(C) Foxp3-TCF1 interaction in human Treg cells was visualized with an in situ proximity ligation assay (PLA). Cells were fixed, and protein-protein interactions were visualized with antibodies directed against Foxp3 and TCF1 as described in the Experimental Procedures. Punctate staining (green) indicates Foxp3-TCF1 interaction as detected by the assay. Nuclei were stained with DAPI. Results depicted are representative of at least three independent experiments.

See also Figure S1.

destruction complex and, thus, rapidly increasing β-catenin protein levels (Staal et al., 2008; Aberle et al., 1997; Reya et al., 2003; Verbeek et al., 1995).

Within the immune system, Wnt signaling has traditionally been studied during lymphocyte development or in the context of hematopoietic stem cell biology (Staal et al., 2008; Verbeek et al., 1995; Reya et al., 2003). Here, we demonstrate that the Wnt-β-catenin-TCF1 module also has an unexpected role as a regulator of Treg cell function.

RESULTS

TCF1 Associates with Foxp3 in Treg Cells

In an unbiased approach to globally identify transcription factors associating with Foxp3, a transcription factor interaction (TF-TF) array was performed (Figure S1A available online; see the Experimental Procedures). The array analysis revealed the association of a member of the Wnt-associated transcription factor TCF family with Foxp3 (Figure 1A). This was confirmed by coimmunoprecipitation analysis with lysates of cells ectopically expressing TCF1 and Foxp3 (Figure 1B, lane 3). TCF1 was found to interact with Foxp3 irrespectively of DNase or EtBr treatment of the lysates, indicating that this association was a protein-protein interaction and not a DNA-mediated interaction (Lai and Herr, 1992). First, we confirmed that components of the Wnt signaling cascade (TCF1, β-catenin, and FZD receptors) were expressed in human Treg cells (Figures S1B–S1D). To evaluate whether endogenous Foxp3 and TCF1 also associate in human Treg cells, we performed an in situ proximity ligation assay (PLA; see the Experimental Procedures). Given that a PLA signal can only be obtained when proteins are in close proximity, this technique enables the detection of direct protein-protein interactions in cells. The association of TCF1 with Foxp3 was detected specifically in the Treg cell nucleus (Figure 1C).

TCF1 Activation Impairs Foxp3 Transcriptional Activity

TCF1 is a key transcription factor that is regulated by canonical Wnt signaling and acts as a transcriptional activator in the presence of β-catenin. To assess whether Wnt signaling modulates Foxp3 transcriptional activity, we used human induced Treg (iTreg) cells to allow for sufficient cell numbers. The iTreg cells used were $CD4^+CD25^{high}$ and $Foxp3^+$, CTLA-4^+, and $GITR^+$ (Figure S2A). To manipulate Wnt signaling in Treg cells, we used BIO, a GSK3 inhibitor widely used to mimic the activation of the Wnt signaling cascade (Sato et al., 2004). Indeed, treatment of human iTreg cells with the Wnt-mimetic BIO resulted in a dose-dependent increase in β-catenin levels and nuclear translocation (Figures S2B–S2D). To assess Foxp3 transcriptional activity in Treg cells, we used the canonical Foxp3 transcriptional target IL-2 as a readout, given that Foxp3 has been reported to directly inhibit *IL2* transcription through promoter binding (Marson et al., 2007; Wu et al., 2006; Gavin et al., 2007). To investigate whether TCF could modulate *IL2* transcription, we treated human Treg cells with BIO. Messenger RNA (mRNA) expression of Axin-2, a ubiquitous TCF1 transcriptional target, was increased, confirming that treatment with BIO indeed activated the Wnt signaling cascade (Figure S2E). BIO treatment of Treg cells also resulted in significantly increased IL-2 mRNA expression (Figure 2A). Foxp3 mRNA expression remained unchanged, demonstrating that this increase occurs independently of changes in Foxp3 expression (Figure S2E). Similarly, intracellular IL-2 protein levels and IL-2 concentrations in the supernatant were significantly increased in mouse and human Treg cells treated with BIO (Figure 2B–2D). Similarly, expression levels of CD25, which are transcriptionally

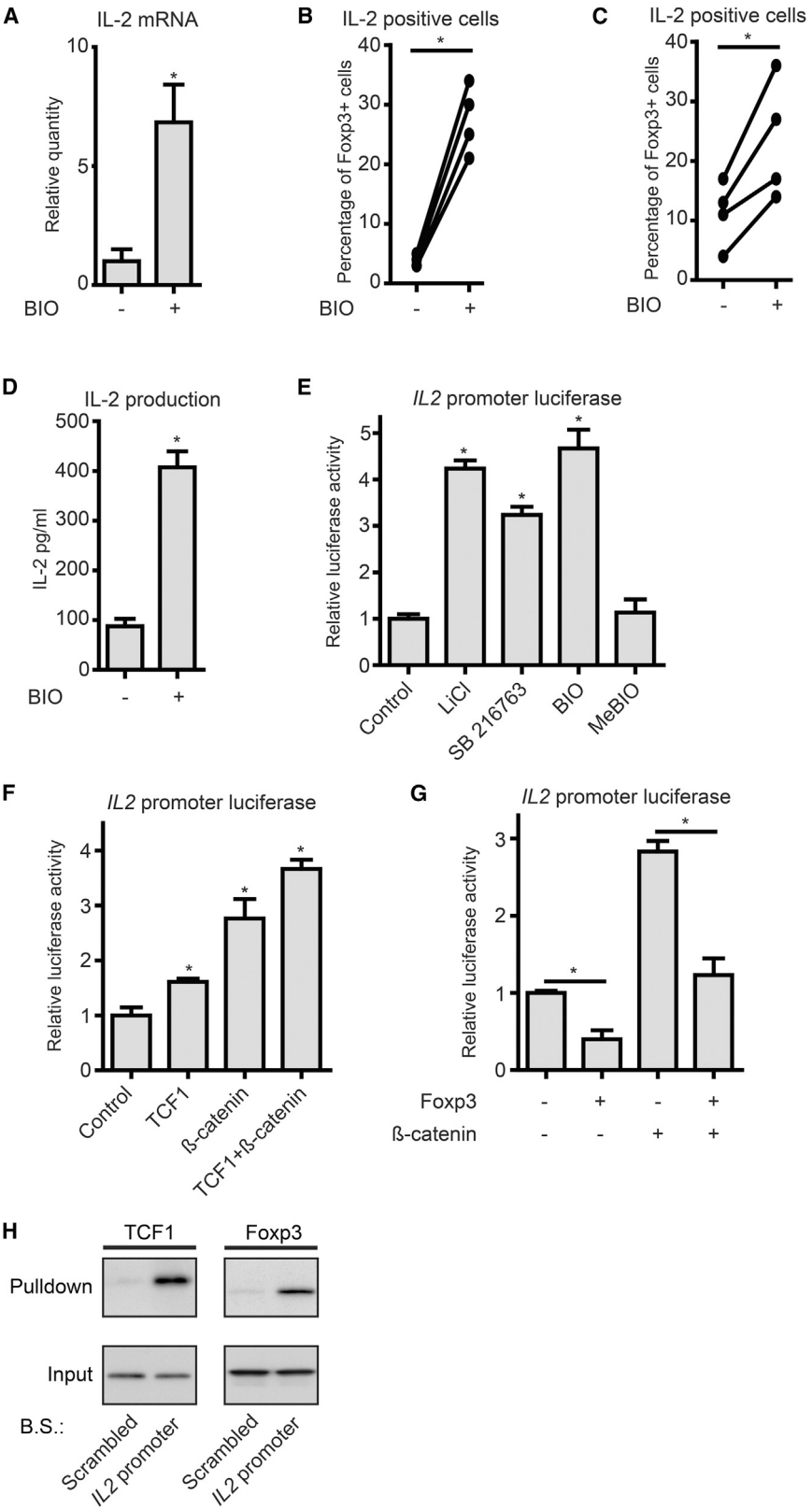

Figure 2. TCF1 Activation Impairs Foxp3 Transcriptional Activity

(A) qRT-PCR analysis of IL-2 mRNA expression in human iTreg cells after incubation with BIO (1 μM) for 18 hr.

(B and C) Freshly isolated mouse splenocytes (B) or human PBMCs (C) were cultured in the presence of anti-CD3 and BIO (1 μM) or MeBIO (1 μM) for 18 hr and stimulated with phosphomolybdic acid and ionomycin for 4 hr, and the percentage of $Foxp3^+$ Treg cells that was $IL\text{-}2^+$ was determined by FACS analysis.

(D) Human iTreg cells were cultured for 18 hr in the presence of anti-CD3/28-coated beads (1:100 beads to cells) in the presence of BIO (1 μM) or MeBIO (1 μM). Supernatants were analyzed for IL-2 levels with multiplex technology.

(E) HEK 293T cells were transfected with an *IL2* promoter luciferase reporter construct, NFAT, and Renilla. Cells were treated with GSK3 inhibitors in order to activate TCF; LiCl (10 mM), SB 216763 (10 μM), BIO, and MeBIO (800 nM) were used as controls.

(F) *IL2* promoter activity was analyzed as in (E), cells were cotransfected with β-catenin and TCF1, and luciferase activity was measured.

(G) *IL2* promoter activity was analyzed in cells cotransfected with β-catenin and Foxp3.

(H) Protein-DNA interaction was analyzed with an oligonucleotide pull-down assay. Lysates of TCF1- or Foxp3-transfected cells were incubated with biotin-labeled oligonucleotide probes containing the TCF and Foxp3 binding site in the human *IL2* promoter. Association was visualized with specific antibodies. B.S., binding site; IP, immunoprecipitation; WB, western blot. Results depicted are representative of at least three independent experiments. Mean + SEM is depicted. See also Figure S2.

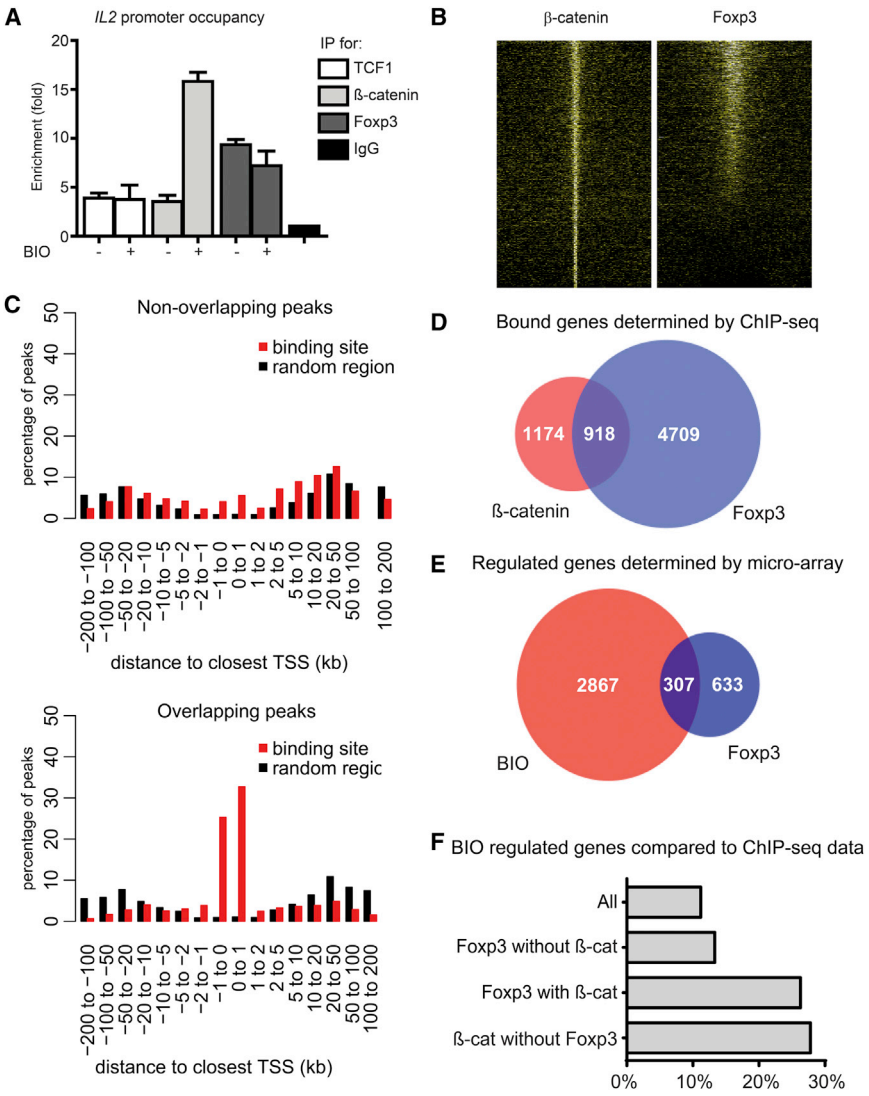

Figure 3. β-Catenin and Foxp3 Share Genomic Binding Sites in Treg Cells

(A) Chromatin immunoprecipitation (ChIP) was applied in order to determine the occupancy of the IL-2 promoter by TCF1, β-catenin, and Foxp3 in human Treg cells pooled from five independent donors treated with BIO (1 μM) or MeBIO (1 μM) for 4 hr. Enrichment relative to IgG control IP samples was determined by qRT-PCR with IL-2-promoter-specific primers.

(B) A heat map of β-catenin and Foxp3 signal intensity in 5,000 bp distance from the center of β-catenin peaks. Each row in the heat map corresponds to the single β-catenin peak. Peaks were sorted according to Foxp3 signal intensity. Each sample was normalized separately to maximum yellow color intensity corresponding to the 0.95th percentile of the read density distribution.

(C) Peak coordinates were compared to the peak coordinates of a human Treg cell Foxp3 ChIP-seq database. The distance of overlapping and nonoverlapping peaks to the closest annotated TSS is depicted.

(D) Overlap of genes bound by β-catenin and Foxp3.

(E) Overlap of genes regulated by BIO in human Treg cells and genes regulated by Foxp3.

(F) Percentage of BIO upregulated genes (from the microarray experiments) in Foxp3- and/or β-catenin (β-cat)-bound genes. All, all genes on the array with a mouse ortholog; IP, immunoprecipitation; TSS, transcription start site. Mean + SEM is depicted.

See also Figure S3.

upregulated by Foxp3, were reduced in human Treg cells treated with BIO (Figure S2F).

To determine whether TCF1 can directly regulate *IL2* promoter activity, we treated *IL2* promoter reporter cells with three chemically distinct GSK3 inhibitors in order to increase β-catenin levels, thereby activating endogenous TCF. All three Wnt mimetics significantly increased *IL2* promoter activity to a similar degree, whereas the MeBIO negative control had no effect (Figure 2E). Increasing the amount of BIO resulted in a dose-dependent increased *IL2* promoter activity (Figure S2G). In addition, *IL2* promoter activity was increased by the ectopic expression of TCF1 and β-catenin (Figure 2F). Foxp3 could significantly repress *IL2* promoter activity, as previously reported (Figure 2G) (Marson et al., 2007; Gavin et al., 2007). However, *IL2* promoter activity was unchanged when both Foxp3 and β-catenin were transfected, indicating that increased β-catenin levels can override Foxp3-mediated suppression of *IL2* promoter activity. Given that TCF1 activation resulted in increased *IL2* promoter activity, we analyzed TCF1 and Foxp3 occupancy of the *IL2* promoter with an oligonucleotide pull-down assay. Lysates of TCF1- or Foxp3-transfected cells were incubated with biotin-labeled oligonucleotide probes containing the predicted TCF and Foxp3 binding site in the human *IL2* promoter, and association was visualized by immunoblotting. Both TCF1 and Foxp3 specifically associated with the IL-2 promoter probe (Figure 2H). Altogether, these data demonstrate that TCF1 activation impairs Foxp3 transcriptional activity.

β-Catenin and Foxp3 Share Common Genomic Binding Sites in Treg Cells

Using chromatin immunoprecipitation (ChIP), we determined whether TCF1, its coactivator β-catenin, and Foxp3 could co-occupy the *IL2* promoter in human Treg cells and whether this association was affected by the activation of Wnt signaling. Quantitative RT-PCR (qRT-PCR) analysis demonstrated that TCF1, β-catenin, and Foxp3 all associate with the *IL2* promoter (Figure 3A). In addition, BIO treatment resulted in a more than 3-fold increase in the amount of β-catenin associating with the *IL2* promoter. To validate these findings and to determine the overlap of β-catenin and Foxp3 genomic binding loci, we performed ChIP-seq analysis for β-catenin in human Treg cells. In total, we identified 3,134 β-catenin-bound regions, of which one-third were located within 1 kb of annotated transcriptional start sites (TSS; Figure S3A). Gene ontology analysis of genes

that show a β-catenin binding site within 5 kb of the TSS displayed a significant enrichment for biological processes, which are associated with T cell function and genes that result in abnormal T-cell-related phenotypes in mice (Figures S3B and S2C).

Notably, 46% of the identified β-catenin-bound regions were located within 1 kb from the published datasets of Foxp3 peaks, indicating a large overlap between β-catenin and Foxp3 target genes, suggesting the coregulation of transcriptional targets (Figure 3B) (Birzele et al., 2011). Moreover, whereas unique β-catenin binding events are located relatively far from the TSS, the overlapping peaks were located close to the TSS, further supporting a functional role in gene transcription for the association of these two factors in Treg cells (Figure 3C). In line with this, we found a large overlap in β-catenin- and Foxp3-bound genes (Figure 3D), suggesting that many transcriptional targets of Foxp3 can be coregulated by β-catenin/TCF1. To gain further insight into the mechanism behind this interplay between Foxp3 and Wnt signaling, we used BIO to activate the Wnt signaling pathway in human Treg cells, and gene expression was evaluated by complementary DNA (cDNA) microarray analysis. Subsequently, BIO-regulated genes were compared to human orthologs of a published dataset of Foxp3-regulated genes (Marson et al., 2007). Approximately 34% of Foxp3-regulated genes were also found to be regulated by Wnt signaling in Treg cells (Figure 3E). Next, we analyzed whether the genes bound by Foxp3 and/or β-catenin were also transcriptionally regulated by BIO. Of the genes bound by Foxp3 and β-catenin, ~26% were regulated by BIO; in contrast, only ~13% of the genes bound exclusively by Foxp3 were BIO regulated (Figure 3F). Altogether, these data demonstrate that a considerable proportion of Foxp3-bound genes are also bound by β-catenin and, correspondingly, regulated by Wnt signaling.

Active Wnt Signaling Abrogates the Suppressive Capacity of Treg Cells

Because we observed that β-catenin/TCF1 could regulate Foxp3 transcriptional targets, we further assessed the role of Wnt signaling in Treg cell function. To analyze this, we performed in vitro suppression assays by culturing sorted human Treg cells along with carboxyfluorescein succinimidyl ester (CFSE)-labeled peripheral blood mononuclear cells (PBMCs). Our results show a Treg:Teff ratio at which Treg-mediated suppression of approximately 50%, given that such a ratio allows for an optimal window for assessing increased or decreased Treg cell function (Figures S4A and S4B). All Wnt mimetics used significantly impaired Treg-cell-suppressive function in vitro, suggesting that Wnt signaling in Treg cells abrogates their suppressive capacity (Figures 4A and S4C). Importantly, there was no direct effect of these inhibitors on PBMC proliferation (Figure 4B). To further confirm that these results were Treg cell specific, Treg cells were preincubated with Wnt mimetics, washed, and analyzed for their suppressive capacity in the absence of inhibitors during the assay. Pretreatment also abrogated Treg-cell-mediated suppression of $CD4^+$ T cell proliferation, confirming our previous observations (Figures 4C and S4D). Comparable results were observed for the $CD8^+$ T cell population (data not shown).

Wnt proteins are unstable and notoriously difficult to purify; however, to determine the effect of direct addition of Wnt protein on Treg-cell-suppressive capacity, we added purified Wnt3a protein or IWP-2 during the suppression assays. IWP-2 is a specific inhibitor of the membrane-bound O-acyltransferase Porcn, which facilitates the palmitoylation of Wnt and thereby prevents Wnt processing and secretion (Willert et al., 2003). The addition of Wnt3a significantly impaired Treg-cell-mediated suppression (Figures 4D and S4E), whereas IWP-2-mediated inhibition of Wnt production resulted in significantly increased Treg-cell-suppressive capacity. Importantly, treatment with Wnt3a or IWP-2 did not directly affect T cell proliferation (Figure 4E). To confirm that these results were a direct effect on Treg cells, we pretreated cells with Wnt3a or IWP-2, and, after washing, Treg cells were cultured with the CFSE-labeled PBMCs for 4 days. Although to a lesser degree, Wnt3a pretreatment inhibited Treg-cell-mediated suppression, validating our previous observations (Figures 4F and S4F). However, IWP-2 pretreatment did not increase Treg-cell-mediated suppression, suggesting that Wnt is most likely produced by the PBMCs in this experimental setup. To further assess the effect of Wnt proteins on Treg cell function, we performed a suppression assay in the presence of FZ8CRD, a soluble truncated Wnt receptor that inhibits Wnt signaling. Again, the suppression of Wnt signaling by the addition of FZ8CRD resulted in increased Treg-cell-suppressive capacity (Figures 4G and S4G). Collectively, these data suggest that Wnt is most likely produced by mononuclear cells during in vitro suppression assays and that the activation of the Wnt pathway diminishes the suppressive functionality of Treg cells.

To assess the role of canonical Wnt signaling in modulating Treg cell functionality in vivo, we used an established mouse colitis model (Mottet et al., 2003). In this model, colitis was induced by the infusion of $CD4^+CD45RB^+$ T cells into immunodeficient *Rag1*$^{-/-}$ mice, and disease severity was diminished by the adoptive transfer of Treg cells. Here, sorted Treg cells from Foxp3-GFP mice were pretreated with BIO (in order to activate TCF) or MeBIO and transferred to donor mice 3 weeks after the transfer of naïve $CD4^+$ cells. An additional 3 weeks after Treg cell treatment, substantial colitis scores were observed in mice that did not receive Treg cells, and infusion with control (MeBIO)-treated Treg cells dramatically decreased colitis scores (Figures 4H and 4I). Importantly, Treg cells pretreated with BIO did not exhibit reduced colitis scores, indicating that TCF activation abrogated Treg cell function in vivo. The percentage of GFP^+ T cells in the spleen and mesenteric lymph nodes (MLNs) were similar in all groups, indicating that treatment with Wnt mimetic did not influence either Treg cell homing or survival (Figures S4H and S4I). Furthermore, AXIN2 expression in sorted GFP^+ Treg cells from the MLNs and spleen of these mice was still increased in BIO-treated Treg cells in comparison to MeBIO-treated Treg, indicating that Wnt signaling was still more active in the BIO-treated Treg cells at the end of the experiment (Figure S4J). To validate that transient stimulation with BIO can indeed affect Treg cell functionally for a sustained period, we transiently treated Treg cells with BIO and cultured them without BIO for 5 days. Subsequently, Treg-cell-mediated suppression was analyzed in an in vitro suppression assay. Suppression of the BIO-pretreated Treg cells was impaired in comparison to MeBIO-treated Treg cells, indicating that transient activation of Wnt signaling

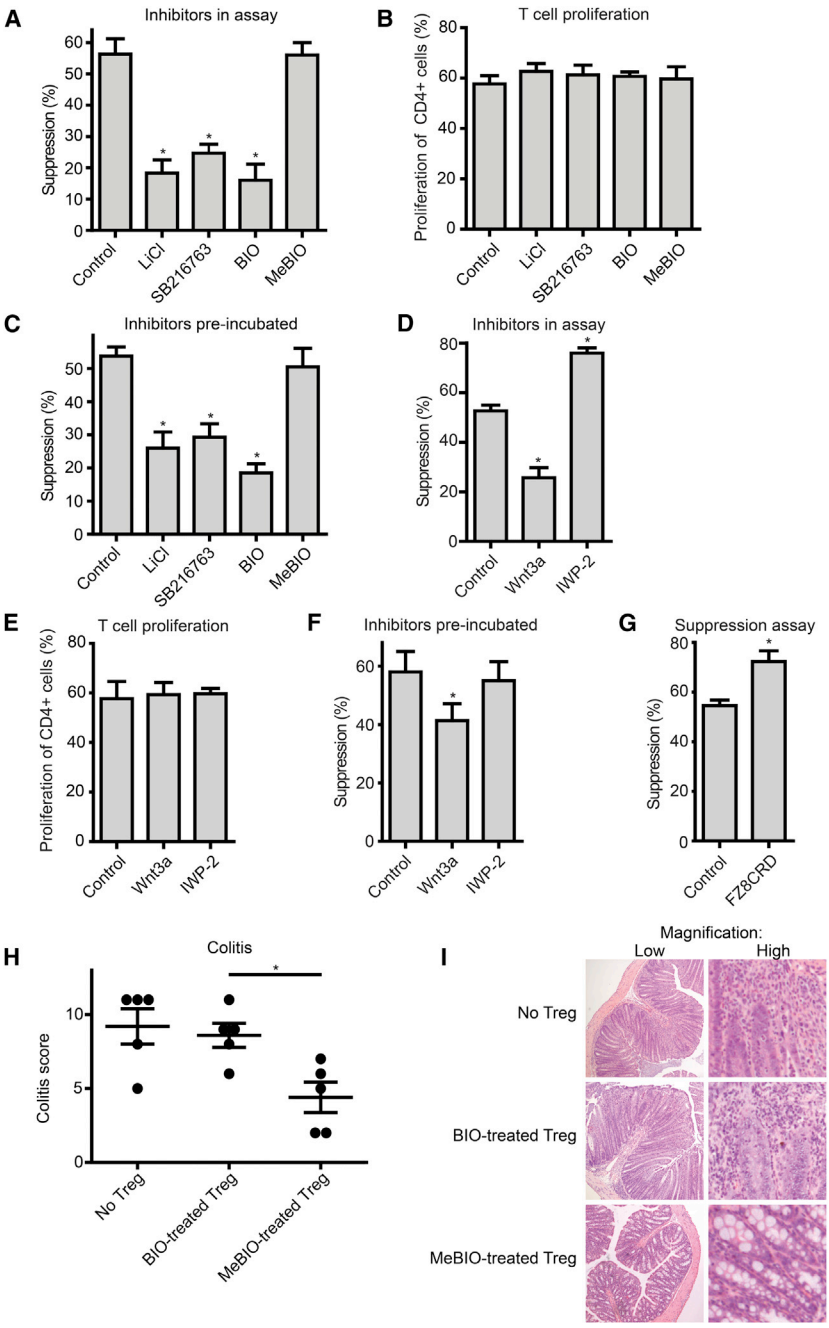

Figure 4. Wnt Signaling Regulates Treg Cell Function

Human T cell suppression assays were performed in order to analyze Treg-cell-mediated suppression. Sorted $CD4^+CD25^{high}CD127^{low}$ Treg cells were co-cultured with CFSE-labeled PBMCs in anti-CD3-coated wells for 4 days. CFSE dilution of CD4s cells was analyzed with FACS.

(A) Suppression by Treg cells in the presence of TCF activators LiCl (5 mM), SB216763 (10 μM), BIO (100 nM), or control MeBIO (100 nM) was analyzed.

(B) Human PBMCs were CFSE labeled and cultured in the presence of 5 mM LiCl, 10 μM SB216763, 100 nM BIO, and 100 nM MeBIO for 4 days in anti-CD3-coated wells. The proliferation of $CD4^+$ cells was analyzed by CFSE dilution.

(C) Sorted Treg cells were preincubated with 10 mM LiCl, 40 μM SB216763, 5 or 10 μM BIO, or 10 μM MeBIO for 1 hr, washed, and functionality analyzed by suppression assay.

(D) Suppression of Treg cells in the presence of Wnt3a (400 ng/ml) or Wnt production inhibitor IWP-2 (2 μM).

(E) Human PBMCs were CFSE labeled and cultured in the presence of 400 ng/ml Wnt3a and 2 μM IWP-2 for 4 days in anti-CD3-coated wells. The proliferation of $CD4^+$ cells was analyzed by CFSE dilution.

(F) Sorted Treg cells were pretreated with Wnt3a (800 ng/ml) or IWP-2 (4 μM) for one hour. Cells were washed and used for suppression assay.

(G) Suppression assay as in (A), cells were cultured in the presence of FZ8CRD.

(H and I) Colitis was induced by infusion of $CD4^+CD45RB^{high}$ cells into immunodeficient mice. At day 21, Treg cells that were preincubated with 10 μM BIO or MeBIO for 1 hr were administered. At day 42, mice were sacrificed, and sections of the colon were analyzed and scored as described in the Experimental Procedures. Mean + SEM is depicted. All experiments were performed in triplicate and for at least three independent donors.

See also Figure S4.

can have a sustained effect on Treg-cell-suppressive function (Figure S4K).

To extend our observations through a genetic approach, we utilized Treg cells isolated from $TCF1^{-/-}$ mutant mice. As previously reported, the number of peripheral $CD4^+$ T cells in TCF1-deficient ($Tcf1^{-/-}$) mice was significantly reduced (Figure S5A) (Staal et al., 2008; Verbeek et al., 1995). However, the percentage of Treg cells was similar in $Tcf1^{-/-}$ mice in comparison to control mice (Figures 5A and S5B). Treg-cell-mediated suppression in vitro was reproducibly and substantially increased in $Tcf1^{-/-}$ Treg cells in comparison to wild-type (WT) Treg cells, demonstrating that the absence of TCF1 positively influences Treg-cell-mediated suppression (Figure 5B). To confirm that these differences in Treg-cell-mediated suppression observed in the $Tcf1^{-/-}$ Treg cells were the result of disrupted Wnt signaling, we repeated the assay in the presence of BIO. As previously observed, Treg-cell-mediated suppression was impaired by BIO treatment and was increased in $Tcf1^{-/-}$ Treg cells (Figures 5C and S5C). However, BIO treatment had no effect on $Tcf1^{-/-}$ Treg cells, demonstrating the specificity of this Wnt mimetic in activating TCF1-mediated transcription and thereby inhibiting Treg cell function.

To further validate these observations, suppression assays were performed with $Apc^{min/+}$ Treg cells. $Apc^{min/+}$ cells have increased β-catenin levels and TCF transcriptional activity because of mutations in *Apc*, a component of the β-catenin destruction complex (Staal et al., 2008; Aberle et al., 1997; Reya et al., 2003; Verbeek et al., 1995). The suppressive capacity of $Apc^{min/+}$ Treg cells was impaired in comparison to $Apc^{+/+}$ Treg cells (Figure 5D).

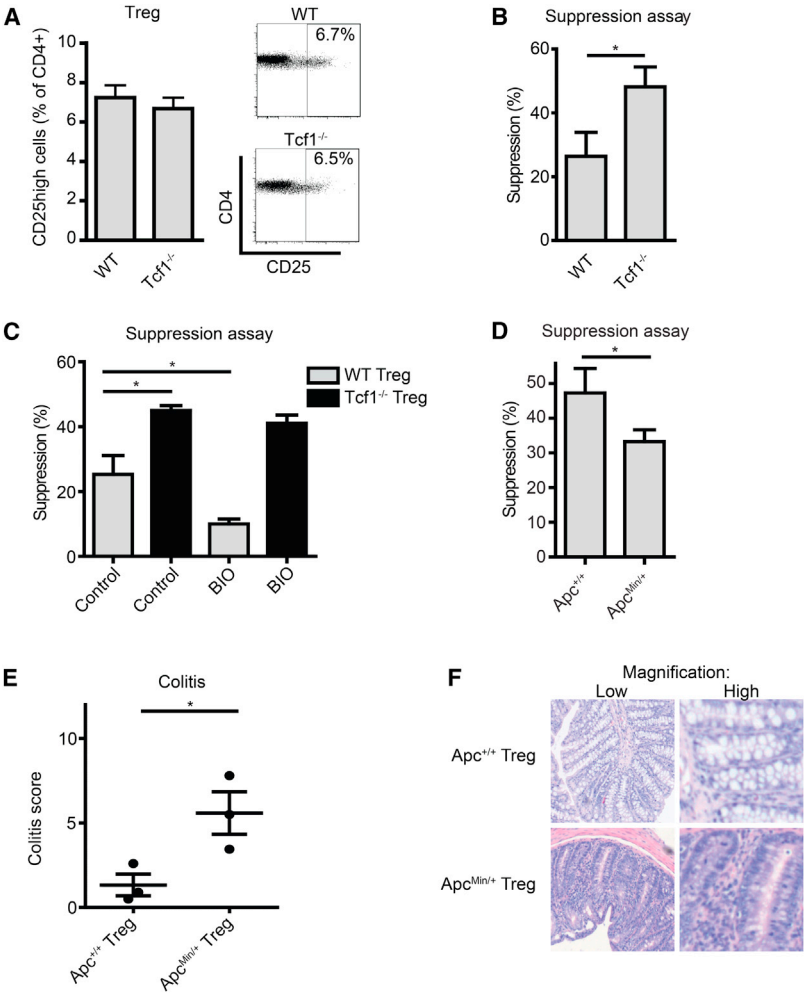

Figure 5. Wnt Signaling Regulates Treg Cell Function

(A) $CD4^+$ splenocytes from both WT and *Tcf1*$^{-/-}$ mice were analyzed for CD25 expression.

(B) In vitro T cell suppression assays were performed in order to analyze Treg cell functionality. Sorted $CD4^+$ $CD25^{high}$ Treg cells from WT or *Tcf1*$^{-/-}$ mice were cocultured with CFSE-labeled WT splenocytes in the presence of soluble anti-CD3 for 4 days. CFSE dilution of $CD4^+$ cells was determined by FACS analysis.

(C) Suppression assay performed as in (B) with sorted $CD4^+CD25^{high}$ Treg cells from WT or *Tcf1*$^{-/-}$ mice that were cultured in the presence or absence of 100 nM BIO.

(D) Suppression assay as in (B) utilizing sorted CD4+ CD25high Treg cells from *Apc*$^{min/+}$ or *Apc*$^{+/+}$ mice. All results depicted are the means + SEM of at least three independent experiments.

(E and F) Colitis was induced by coinfusion of $CD4^+$ $CD45RB^{high}$ cells with $CD4^+CD25^{high}$ *Apc*$^{min/+}$ or *Apc*$^{+/+}$ Treg cells into immunodeficient mice. At day 42, mice were sacrificed, and colitis scores were analyzed. Sections of the colon were analyzed and scored as described in the Experimental Procedures. Mean + SEM is depicted. All experiments were performed in triplicate and for at least three independent donors.

See also Figure S5.

To extend these observations in vivo, we performed the mouse colitis model again with *Apc*$^{min/+}$ Treg cells that were cotransferred with naïve WT CD4 T cells. As shown in Figures 5E and 5F, 6 weeks after transfer colitis, scores were significantly increased in the group receiving *Apc*$^{min/+}$ Treg cells in comparison to the group that had received Treg cells derived from WT mice. Altogether, these data demonstrate that increased Wnt signaling also abrogates Treg cell function in vivo.

Increased Wnt3a Production Is Associated with Arthritis

Given that the addition of Wnt3a significantly abrogated Treg cell function, Wnt3a expression was analyzed in human CD4 T cells upon activation. We observed the expression of Wnt3a in $CD4^+$ T cells, and T cell activation with anti-CD3 and anti-CD28 resulted in a 3-fold increase in Wnt3a mRNA expression (Figure 6A). Treg cells are known to be present in high numbers in the joints of arthritis patients; however, they are unable to control local inflammation (Lindley et al., 2005; Viglietta et al., 2004; Ehrenstein et al., 2004). Furthermore, we have previously reported that Treg-cell-mediated suppression is reduced when cocultured with synovial fluid mononuclear cells (SFMCs) from arthritis patients in comparison to coculture with PBMCs (Wehrens et al., 2011). Because we observed that Wnt3a significantly impairs Treg cell function, we wanted to determine whether mononuclear cells at an inflammatory locus may produce Wnt3a and thereby inhibit Treg cell functionality. PBMCs and matched SFMCs were isolated from five juvenile idiopathic arthritis patients, and Wnt3a mRNA levels were compared. We observed a 10-fold increase of Wnt3a in SFMCs in comparison to PBMCs from the same patient (Figure 6B). To determine whether the inhibition of Wnt production by SFMCs would therefore result in increased Treg-cell-mediated suppression, we performed a suppression assay with SFMCs by using donor-matched Treg cells in the presence of the Wnt production inhibitor IWP-2. As previously reported, Treg-cell-mediated suppression was reduced in Treg cells from juvenile idiopathic arthritis (JIA) patients in comparison to healthy controls (Figures 6C and S5D) (Wehrens et al., 2011). Strikingly, when Wnt production was inhibited, Treg-cell-mediated suppression in patient cells was comparable to that of healthy controls. These data indicate that Wnt3a production at the site of (auto)inflammation may locally dampen Treg-cell-mediated suppression in these patients.

Because we observed that Wnt production was increased by mononuclear cells of JIA patients and that the inhibition of Wnt production could restore Treg-cell-mediated suppression, we sought to modulate Wnt activation in a murine arthritis model. To this end, we used a proteoglycan-induced arthritis mouse model (Glant and Mikecz, 2004; Roord et al., 2008). Importantly, this model is Treg dependent, given that the depletion of Treg cells results in significantly increased arthritis scores (Roord et al., 2008). Arthritis was induced by proteoglycan injections, and arthritis scores were analyzed three times per week by a visual scoring system of redness, swelling, and deformities of

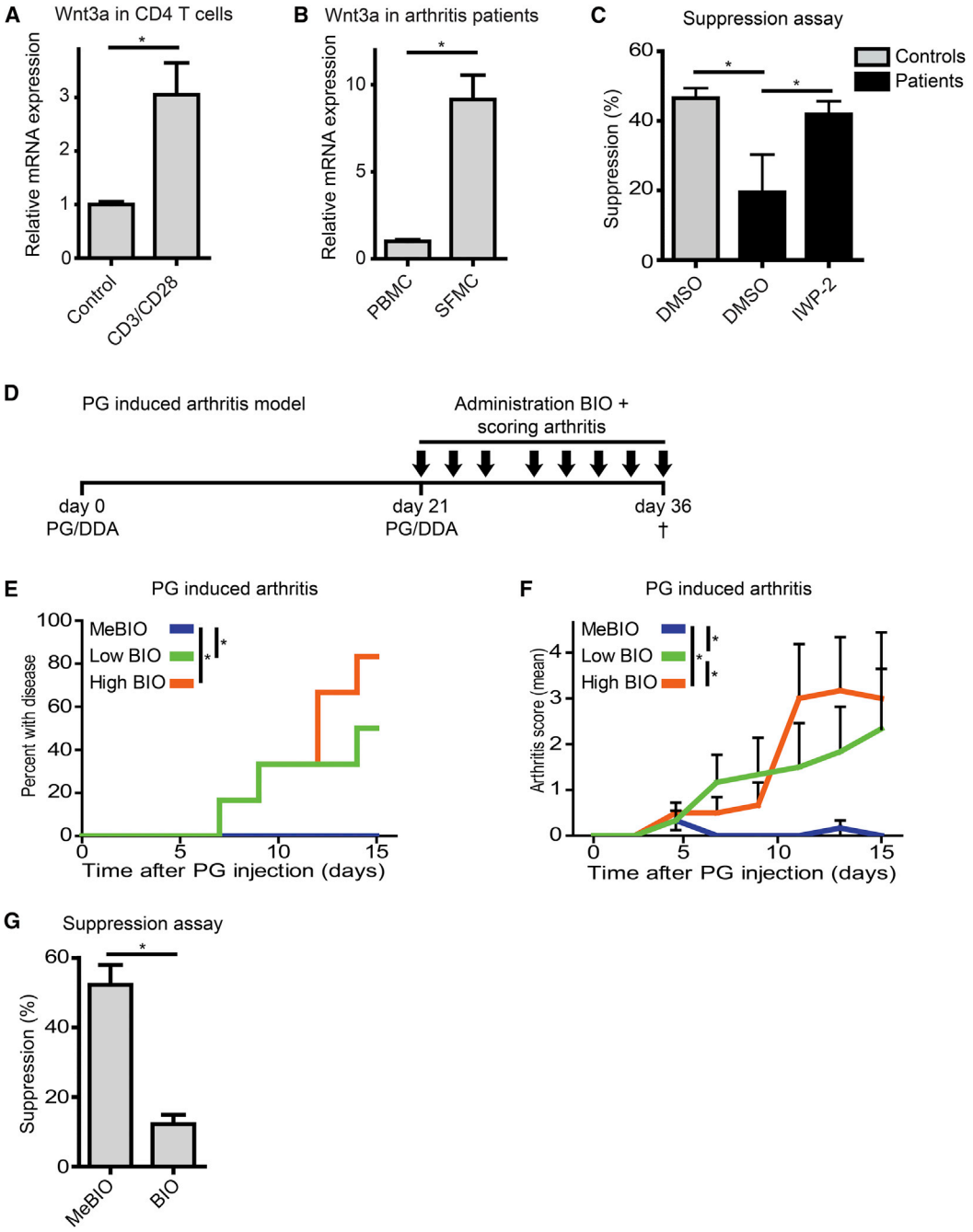

Figure 6. Increased Wnt3a Production Is Associated with Arthritis

(A) Wnt3a mRNA levels were analyzed by qRT-PCR from $CD4^+$ T cells that were sorted from human PBMCs and cultured overnight in the absence or presence of anti-CD3- and anti-CD28-coated beads.

(B) Wnt3a mRNA levels were determined in PBMCs or SFMCs from five different JIA patients.

(C) In vitro T cell suppression assays were performed in order to analyze Treg cell functionality. Sorted $CD4^+CD25^{high}$ Treg cells isolated from healthy control PBMCs or arthritis patient SFMCs were cocultured with matched CFSE-labeled PBMCs or SFMCs in the presence of anti-CD3 for 4 days. IWP-2 was added in order to inhibit Wnt production. CFSE dilution of $CD4^+$ cells was determined by FACS analysis.

(D) Arthritis was induced by two injections of PG in DDA on day 0 and day 21. Mice were treated with 6 mg/kg BIO or MeBIO twice a week or 2 mg/kg BIO three times a week, and disease was scored (six mice per group) as described in the Experimental Procedures.

(E) Mice with an arthritis score of at least 2 are depicted.

(F) Mean arthritis scores are shown.

(G) Mice I.P. injected with 6 mg/kg BIO or MeBIO were sacrificed 18 hr after injection. Treg cells isolated from the spleen were cocultured with CFSE-labeled splenocytes in the presence of anti-CD3 for 4 days, and Treg-cell-mediated suppression was determined by CFSE dilution. Mean + SEM is depicted.

See also Figure S5.

the paws (Glant and Mikecz, 2004). To mimic Wnt signaling, mice were subjected to intraperitoneal (I.P.) injections with low BIO (2 mg/kg, three times per week), high BIO (6 mg/kg, two times per week), or MeBIO (6 mg/kg, two times per week) as a control (Figure 6D). In these experiments, relatively young (16 weeks old) mice that do normally not develop arthritis after two proteoglycan (PG) injections under these experimental conditions were used. As expected, no mice developed arthritis in the control group (MeBIO). However, arthritis was observed in five out of six mice that received high BIO and in three out of six mice of the low BIO group, demonstrating a dose-dependent effect of Wnt mimetic on disease scores (Figures 6E and 6F). Importantly, mice that did not receive PG but were treated with high BIO did not develop arthritis (data not shown). No significant differences were observed in $Foxp3^+$ percentages or mean fluorescence intensity in the spleen, again demonstrating that BIO treatment does not modulate either the number of $Foxp3^+$ Treg cells or Foxp3 expression levels (Figures S5E and 5F).

To confirm that the increased arthritis scores in BIO-treated mice could be the result of impaired Treg cell functionality, we performed an ex vivo suppression assay. Foxp3-GFP mice were sacrificed 18 hr after I.P. injection with BIO or MeBIO. Equal numbers of GFP^+ Treg cells were isolated from the spleen, and Treg-cell-mediated suppression of untreated Teff cell proliferation was analyzed. The suppressive capacity of Treg cells from BIO-treated mice was significantly impaired in comparison to control-treated mice, indicating that the systemic activation of Wnt signaling indeed abrogates Treg cell function (Figures 6G and S5G). Altogether, these mouse models demonstrate that Wnt signaling can abrogate Treg-cell-mediated suppression in vivo, which can result in the onset of arthritis.

T cell activation and proliferation is necessary for clearing infections; however, at the site of inflammation, activated T cells have been reported to directly interact with Treg cells (Mempel et al., 2006; Stern and Smith, 1986). Because extensive or prolonged Treg cell activity would be detrimental for the resolution of infection, we propose a model in which Wnt production by mononuclear cells could modulate the strength of the immune response. Here, Wnt-mediated activation of FZD receptors expressed on Treg cells could dampen Treg-cell-mediated immune suppression through the inhibition of Foxp3 transcriptional output. However, when uncontrolled, this would potentially contribute to the development of autoimmunity (Figure S6).

DISCUSSION

Although Wnt signaling has traditionally been studied in the context of thymocyte development and stem cell biology (Staal et al., 2008; Verbeek et al., 1995; Reya et al., 2003), we present data demonstrating an important functional role in immune regulation. The role of Wnt proteins in regulating peripheral T cell function remains poorly understood. In recent studies demonstrating that the Wnt pathway can modulate $CD8^+$ T cell responses, TCF1 deficiency was shown to limit the proliferation of $CD8^+$ effector T cells and impair differentiation toward a central memory phenotype (Zhou et al., 2010; Gattinoni et al., 2009). Furthermore, TCF1 was found to be a T-cell-specific tumor suppressor for the development of lymphomas because of the repression of LEF1 (Tiemessen et al., 2012). The ablation of β-catenin in mouse intestinal dendritic cells impaired their ability to induce Treg cells (Manicassamy et al., 2010), although a single study reported that retroviral transduction of a stabilized β-catenin mutant resulted in increased Treg cell survival (Ding et al., 2008). However, continuous high amounts of β-catenin are not favorable, and it has been shown that the expression of stabilized β-catenin in thymocytes can result in the development of thymic lymphomas (Guo et al., 2007). Therefore, interpreting experiments with the overexpression of stabilized β-catenin mutants can be difficult. Here, we show that Wnt signaling directly modulates Foxp3 activity and thereby Treg cell function. We used (1) recombinant Wnt3a, (2) a Wnt production inhibitor, (3) a Wnt antagonist, (4) multiple distinct GSK3 inhibitors (Wnt mimetics), and (5) $Apc^{min/+}$ and $TCF1^{-/-}$ mice to manipulate Wnt signaling in vitro and in vivo and thereby robustly studied the mechanism underlying these observations.

The role of Treg cells in autoimmunity has been extensively studied, and, although IPEX is the result of severely reduced number of Treg cells (Wildin et al., 2001; Bennett et al., 2001), the observation that, in most autoimmune diseases, the number of Treg cells is normal or even increased suggests that here these Treg cells are in some way dysfunctional (Buckner, 2010; Yan et al., 2010; Han et al., 2009). Treg-cell-suppressive capacity is reported to be severely impaired in a variety of autoimmune diseases, including psoriasis, multiple sclerosis, type 1 diabetes, systemic lupus, and rheumatoid arthritis (Lindley et al., 2005; Viglietta et al., 2004; Ehrenstein et al., 2004). Furthermore, Treg-cell-mediated suppression was reported to be reduced when cocultured with SFMCs from arthritis patients in comparison to PBMCs, suggesting that SFMCs can produce factors that abrogate Treg cell functionality (Wehrens et al., 2011). Although there are potentially multiple mechanisms by which Treg cell suppressive capacity could be impaired, we demonstrate here that Wnt3a production provides a possible explanation. The suppressive capacity of Treg cells was increased when PBMCs were cultured in the presence of the Wnt production inhibitor IWP-2, suggesting that PMBCs can produce Wnt proteins, thereby inhibiting Treg cell function. In support of this, we established that $CD4^+$ T cells do indeed produce Wnt3a, and this was significantly increased upon activation. We also demonstrate that mononuclear cells in the synovial fluid of JIA patients produce almost ten times more Wnt3a than PBMCs from the same donor. When Wnt production was inhibited in SFMCs, Treg-cell-mediated suppression was comparable to that of healthy controls. Altogether, we suggest that dysregulated Wnt production in the synovium could inhibit Treg cell function, leading to an uncontrolled immune response and inflammation, as observed in juvenile idiopathic arthritis.

Using ChIP-seq and microarray experiments, we demonstrate that Wnt signalling (β-catenin/TCF1) and Foxp3 share many transcriptional targets and bind to common genomic regions. Recently, Samstein et al. (2012) demonstrated that Foxp3 exploits a pre-existing enhancer landscape. Foxp3 was found to bind preaccessible enhancers that were already occupied by Foxp3 binding partners. Our data suggest that Foxp3 might have a similar relationship with TCF1-regulated enhancer elements.

We demonstrate that activating Wnt signaling in Treg cells with LiCl significantly abrogates their suppressive capacity. Several studies have reported that Li intake is strongly correlated with an increased predisposition for autoimmunity. Li salts are used for the treatment of manic depression, and case studies reporting the onset of psoriasis after treatment with Li date as far back as 1972. The incidence of psoriasis secondary to Li treatment has been reported to be from 1.8% to 6% (Chan et al., 2000; Sarantidis and Waters, 1983). In addition to psoriasis, there are multiple reports of onset of autoimmune thyroid disease as a result of Li treatment (Calabrese et al., 1985; Thompson and Baylis, 1986). Furthermore, rats immunized with rat thyroglobulin and treated with Li showed significantly increased antithyroglobulin levels in comparison to untreated littermates (Hassman et al., 1985). Given that we have demonstrated that LiCl treatment inhibits Treg-cell-mediated suppression in multiple models, it is possible that increased autoimmunity phenotypes observed in Li-treated patients are caused by abrogated Treg cell function.

Collectively, these data demonstrate that Wnt signaling can modulate Treg-cell-mediated suppression. Therefore, manipulating Wnt signaling could provide a therapeutic strategy for controlling inappropriate immune responses and autoimmune diseases.

EXPERIMENTAL PROCEDURES

Antibodies, DNA Constructs, and Reagents

The following human antibodies were used: mouse anti-Foxp3 clone PCH101 for fluorescence-activated cell sorting (FACS) analysis (eBioscience), mouse anti-hemagglutinin (HA) clone 12CA5 (Santa Cruz Biotechnology), mouse anti-FLAG (Sigma-Aldrich), mouse anti-β-catenin (BD Biosciences), rabbit anti-β-catenin (Cell Signaling Technology), rabbit anti-TCF1 (Cell Signaling), anti-CD4 (BioLegend), anti-CD25, anti-CD127, and anti-CD8 (all BD Biosciences). The following mouse antibodies were used: anti-TCR, anti-CD4, anti-CD25, and anti-CD8 (all BD Biosciences). HA-Foxp3 was cloned from MIGR1-Foxp3 (kindly provided by S. Sakaguchi) (Hori et al., 2003) into pMT2 containing a HA-tag-generating pMT2-HA-Foxp3. FLAG-Foxp3 and pRSV-NFATC/A were described previously (van Loosdregt et al., 2010). *IL2* promoter luciferase (Panomics) has been described previously. pcDNA3 (Invitrogen), LiCl (Sigma-Aldrich), SB 216763 (Sigma-Aldrich), BIO (Calbiochem), MeBIO (Calbiochem), and IWP-2 (Sigma-Aldrich) were all used in this study. Recombinant Wnt3a protein was produced in *Drosophila* S2 cells and purified with blue sepharose affinity and gel filtration chromatography as described previously (Willert et al., 2003).

TF-TF Interaction Array

Human embryonic kidney (HEK) 293T cells were transfected with HA-Foxp3 or empty vector. Nuclear extract were prepared 48 hr after transfection, and the array was screened according to the manufacturer's protocol (Panomics). Immunoprecipitation was performed with anti-HA-coupled beads (Sigma-Aldrich).

Cell Culture and Luciferase Assays

HEK 293T cells were cultured and transfected as described previously (Beekman et al., 2012) In short, cells were maintained in Dulbecco's modified Eagle's medium (Invitrogen) supplemented with 8% heat-inactivated fetal calf serum (FCS), penicillin, and streptomycin (Invitrogen) at 37°C and 5% CO_2. Cells were transfected with a mixture of 1.5 μg DNA and 7.5 μl polyethylenimine overnight. For the luciferase assay, cells were transfected with 1.0 μg IL-2 promoter luciferase reporter with 0.5 μg of pMT2-Foxp3, pcDNA3-NFATC/A, or pcDNA3, 7 μg pMT2 empty vector, and 0.05 μg pRLTK Renilla (Promega) in order to normalize for transfection efficiency. Cells were transfected in a six-well plate, and, 3 days after transfection, the cells were lysed in 50 μl passive lysis buffer, insoluble cell debris was spun down, and the supernatant fraction was assayed for luciferase activity with a Dual-Luciferase Reporter Assay System (Promega).

Oligonucleotide Pull-Down Assay

In vitro translated TCF1 was incubated at 30°C for 10 min with either 0.5 nmol of the 5′-biotinylated double-stranded binding sites. The following biotinylated primers were utilized: Scrambled, GCAGGATCCCATGGGC; IL-2 promoter, AAGAATAAATGTTTAGATTTGTTGATAAACAGGAAGTGT. Subsequently, oligonucleotides were coupled to streptavidin-agarose beads (Sigma-Aldrich). After incubation, the biotinylated oligonucleotide-coupled streptavidin beads were washed at least six times with low-salt buffer containing 150 mM NaCl and denatured in SDS sample buffer before being run on an SDS-acrylamide gel. Then, the separated proteins were immunoblotted for TCF1 with specific antibodies.

Proximity Ligation Assay

PLA detection was performed as described previously (van Loosdregt et al., 2011). In short, iTreg cells were fixed with 3% paraformaldehyde for 10 minutes. Subsequently, cells were washed three times with PBS and blocked for 30 minutes at 22°C in PBS containing 10% normal donkey serum, 0.5% BSA, and 0.5% saponin. After blocking, cells were incubated for 60 min at 22°C with mouse anti-Foxp3 and rabbit anti-TCF1 in PBS containing 10% normal donkey serum, 0.5% BSA, and 0.5% saponin. Cells were washed three times with PBST (0.05% Tween) and incubated with the secondary mouse PLUS and rabbit MINUS antibodies for 1.5 hours at 37°C in the dark. Cells were washed three times in PBST before detection of the probe with the in situ PLA detection kit (Abnova). Cells were analyzed with a 63× objective on a Zeiss LSM 710 fluorescence microscope.

Chromatin Immunoprecipitation

ChIP was performed as described previously (Engelen et al., 2011). An iTreg cell pool of five different donors was crosslinked with 2 mM disuccinimidyl glutarate (Thermo Fisher Scientific) and 1% formaldehyde. Cells were lysed in preimmunoprecipitation buffer (10 mM Tris, 10 mM NaCl, 3 mM $MgCl_2$, and 1 mM $CaCl_2$), chromatin was prepared, and ChIP was performed according to the Millipore online protocol with 15 μg of antibodies against TCF1 or rabbit IgG as a control. The following primers were used for analysis: forward TTGGCCCTAATCTGACCTTTT and reverse GGTGCATAGGCAGGAATGAT.

For ChIP-seq, immunoprecipitated chromatin was sheared and end repaired, sequencing adaptors were ligated, and the library was amplified by ligation-mediated PCR (LMPCR). After LMPCR, the library was purified and checked for the proper size range and for the absence of adaptor dimers on a 2% agarose gel, barcoded, and sequenced on a SOLiD/AB sequencer in multiplexed way in order to produce 50 bp reads. Sequencing reads were mapped against the reference genome (hg19 assembly, National Center for Biotechnology Information build 37) with the Burrows-Wheeler Alignment Tool. Multiple reads mapping to the same location and strand were collapsed to single read, and only uniquely placed reads were used for peak calling. Cisgenome was used for peak calling from the ChIP-seq data.

In Vitro Suppression Assays

Human

$CD4^+CD25^{high}CD127^{low}$ Treg cells were sorted from human PBMCs and cocultured with PBMCs labeled with 2 μM CFSE (at ratios of 1:10, 1:5, 1:2, and 1:1) in anti-CD3 (clone OKT3)-coated 96-well plates. Cells were cultured for 4 days in RPMI medium supplemented with 10% FCS, 100 U/ml penicillin, 100 μg/ml streptomycin, and 5×10^{-5} M 2-β mercaptoethanol. Proliferation of $CD4^+$ cells was determined by measuring CFSE dilution with a FACSCANTO Analyzer (BD Biosciences). Suppression was determined by a comparison of the percentage of proliferating cells with or without Treg cells.

Mouse

CD4 T cells were isolated by magnetic-activated cell sorting from mice spleen, and $CD4^+CD25^+$-sorted cells were added to CFSE-labeled splenocytes at a ratio of 1:5. Cells were cultured in Iscove's modified Dulbecco's medium supplemented with 10% FCS, 2 mM L-glutamine, 100 U/ml penicillin, 100 μg/ml streptomycin, and 5×10^{-5} M 2-mercaptoethanol in the presence of 1 μg/ml soluble anti-CD3 (clone 145-2C11, BD Pharmingen) for 4 days. To determine

the suppression of proliferation the CFSE dilution within the CD4 T cells, we analyzed cell population with FACS.

Quantitative PCR

qPCR was performed as described previously (van Loosdregt et al., 2013). mRNA was isolated with trizol according to the manufacturer's protocol (Invitrogen), cDNA synthesis was performed with an iScript cDNA Synthesis Kit (Bio-Rad). cDNA samples were amplified with SYBR Green Supermix (Bio-Rad) in a MyiQ Single-Color Real-Time PCR Detection System (Bio-Rad) according to the manufacturer's protocol. The primers used for qPCR were: β2M forward: CCAGCAGAGAATGGAAAGTC reverse: GATGCTGCTTA CATGTCTCG Wnt3a forward: TCACGCTCTCGGGGCGGACTC reverse: ACA GCCAGCGACCACCAGATCGG Axin2 forward: AGCCAAAGCGATCTACAA AAGG reverse: GGTAGGCATTTTCCTCCATCAC mAxin2 forward: AAGCCC CATAGTGCCCAAAG reverse: GGGTCCTGGGTAAATGGGTG FZD1 forward: GCTGCGGAGAGTTGCGCTCTCTA reverse: CGAGCCCAAGCCGCTTTCG FZD3 forward: CGCCGGGGTCTGAGGATAGCA reverse: ACATGGGGCAC ATTTGGCCAACA FZD6 forward: TCAGCGGCTTGTATCTTGTGCCA reverse: TGGTCGAGCTTTTGCTTTTGCCTGA FZD7 forward: CTCTCCCAACCGCCT CGTCGCA reverse: ACAGAGGCCCAGGGACGAAAGC FZD8 forward: GCA TGGAGTGGGGTTACCTGTT reverse: ATGCCCTTACACAGCGGCAC FZD9 forward: CACCGTGGCGGTCTTCATGCTCAA reverse: CGGCCAGCTGCTA TCTTGCGGT FZD10 forward: CACCTGGGCGCTCCAAGAAGAGG reverse: ATACCGGGAAGCGAGGGAAGC TCF1 forward: GTGACAAAAGGCCCCTTT CCGAC reverse: CACAGGCCTGGCTGATTCCTTGT TCF4 forward: TACAGA GGCATGCCACCAGGACT reverse: TGGTGTCAGGTCCTCATCGTCA β-catenin forward: GAAGGTGTGGCGACATATGCAGCT reverse: ATCCAAGGGGTT CTCCCTGGGC. In order to quantify the data, the comparative Ct method was used. Relative quantity was defined as $2^{-\Delta\Delta Ct}$, and β2-microglobulin was used as a reference gene.

Transgenic Mice

C57Bl/6 *Tcf1*$^{-/-}$ mice were originally described by Verbeek et al. (1995). All mice were kept in the specified pathogen-free breeding section of the Leiden University Medical Center.

Proteoglycan-Induced Arthritis Mouse Model

PG was purified from human articular cartilage and removed during knee joint replacement surgery by 4 M guanidinium chloride extraction, and the human glycosaminoglycan side chains were depleted by digestion with chondroitinase ABC. Arthritis was induced in BALB/c mice by two I.P. injections of 0.4 mg human deglycosylated PG in 2 mg of the synthetic adjuvant dimethyl dioctadecyl ammonium bromide (DDA, Sigma-Aldrich) on days 0 and 21. Mice were I.P. injected with low BIO (2 mg/kg, three times per week), high BIO (6 mg/kg, two times per week), or MeBIO (6 mg/kg two times per week) as a control from day 21. The onset and severity of arthritis were assessed three times a week in a blinded fashion by a visual scoring system as described previously (Roord et al., 2008). In brief, the degree of joint swelling, redness, and deformation of each paw (scored from zero to four) was determined to express a total arthritis score. The mice were kept in the animal facility of the Utrecht University under regular conditions. The experiments were approved by the Animal Experiment Committee of Utrecht University.

Induced Colitis Mouse Model

Colitis experiments were performed as previously described (Zaiss et al., 2013). *Rag1*$^{-/-}$ mice were kept in the animal facility of the Utrecht University under specific pathogen-free conditions. The experiments were approved by the Animal Experiment Committee of Utrecht University. Immunodeficient mice were injected with 3×10^5 $CD4^+CD45^{high}$ cells in order to induce colitis. After 21 days, 3×10^5 Treg cells isolated from Foxp3-GFP mice were pretreated with 10 μM BIO or MeBIO for 1 hr, washed, and injected intravenously via the lateral tail vein. The mice were sacrificed 3 weeks later, and colons were fixed in formalin for 24 hr, embedded in paraffin, cut, and stained by hematoxylin and eosin. Scoring was performed according to Berg et al. (1996). In brief, grade 0 is equivalent to no infiltration of mononucleated cells. Grade 1 is equivalent to few foci of mononucleated cells and only a slight depletion of goblet cells. Grade 2 is equivalent to many foci of mononucleated cells, infiltration in the lamina propria but not yet in the submucosa, and a diminished numbers of goblet cells. Grade 3 is equivalent to strong infiltration, also in the submucosa, epithelial hyperplasia, and a number of goblet cells strongly diminished. Grade 4 is equivalent to transmural infiltration of mononucleated cells, strong epithelial hyperplasia and strong goblet cell depletion. Each segment of the colon (ascending, transverse, or descending) was given an individual score, and the sum of these scores gave the overall histological score for each mouse. The percentage of GFP^+ cells in the spleen and MLNs were analyzed by FACS.

Statistical Analysis

Statistical analysis was performed with the Mann-Whitney test (GraphPad Prism). $p < 0.05$ was considered statistically significant.

ACCESSION NUMBERS

The ChIP-seq data presented in this study were deposited in the NCBI GEO under accession number GSE49199.

SUPPLEMENTAL INFORMATION

Supplemental Information contains six figures and can be found with this article online at http://dx.doi.org/10.1016/j.immuni.2013.07.019.

ACKNOWLEDGEMENTS

The authors thank M. Klein for technical assistance and S. Sakaguchi, B. Burgering, M. van de Wetering, and A. Banham for providing us with plasmids. V.F. was supported by a grant from the Dutch Rheumatism Foundation (Reumafonds). M.M.T. was supported by the American Institute for Cancer Research (AICR) and VENI-ZonMW. R.v.B. was supported by the Center for Translational Molecular Medicine. F.J.T.S. was supported by a TOP grant from the Netherlands Organisation for Health Research and Development, KiKA, and the AICR. M.M.M. was supported by Dutch Cancer Society (2006-3508), Utrecht University (High Potential Programme), and the European Research Council (starting grant 242958).

Received: July 17, 2012
Accepted: April 26, 2013
Published: August 15, 2013

REFERENCES

Aberle, H., Bauer, A., Stappert, J., Kispert, A., and Kemler, R. (1997). beta-catenin is a target for the ubiquitin-proteasome pathway. EMBO J. *16*, 3797–3804.

Beekman, J.M., Vervoort, S.J., Dekkers, F., van Vessem, M.E., Vendelbosch, S., Brugulat-Panès, A., van Loosdregt, J., Braat, A.K., and Coffer, P.J. (2012). Syntenin-mediated regulation of Sox4 proteasomal degradation modulates transcriptional output. Oncogene *31*, 2668–2679.

Bennett, C.L., Christie, J., Ramsdell, F., Brunkow, M.E., Ferguson, P.J., Whitesell, L., Kelly, T.E., Saulsbury, F.T., Chance, P.F., and Ochs, H.D. (2001). The immune dysregulation, polyendocrinopathy, enteropathy, X-linked syndrome (IPEX) is caused by mutations of FOXP3. Nat. Genet. *27*, 20–21.

Berg, D.J., Davidson, N., Kühn, R., Müller, W., Menon, S., Holland, G., Thompson-Snipes, L., Leach, M.W., and Rennick, D. (1996). Enterocolitis and colon cancer in interleukin-10-deficient mice are associated with aberrant cytokine production and CD4(+) TH1-like responses. J. Clin. Invest. *98*, 1010–1020.

Birzele, F., Fauti, T., Stahl, H., Lenter, M.C., Simon, E., Knebel, D., Weith, A., Hildebrandt, T., and Mennerich, D. (2011). Next-generation insights into regulatory T cells: expression profiling and FoxP3 occupancy in Human. Nucleic Acids Res. *39*, 7946–7960.

Buckner, J.H. (2010). Mechanisms of impaired regulation by CD4(+)CD25(+) FOXP3(+) regulatory T cells in human autoimmune diseases. Nat. Rev. Immunol. *10*, 849–859.

Calabrese, J.R., Gulledge, A.D., Hahn, K., Skwerer, R., Kotz, M., Schumacher, O.P., Gupta, M.K., Krupp, N., and Gold, P.W. (1985). Autoimmune thyroiditis in manic-depressive patients treated with lithium. Am. J. Psychiatry *142*, 1318–1321.

Chan, H.H., Wing, Y., Su, R., Van Krevel, C., and Lee, S. (2000). A control study of the cutaneous side effects of chronic lithium therapy. J. Affect. Disord. *57*, 107–113.

Ding, Y., Shen, S., Lino, A.C., Curotto de Lafaille, M.A., and Lafaille, J.J. (2008). Beta-catenin stabilization extends regulatory T cell survival and induces anergy in nonregulatory T cells. Nat. Med. *14*, 162–169.

Ehrenstein, M.R., Evans, J.G., Singh, A., Moore, S., Warnes, G., Isenberg, D.A., and Mauri, C. (2004). Compromised function of regulatory T cells in rheumatoid arthritis and reversal by anti-TNFalpha therapy. J. Exp. Med. *200*, 277–285.

Engelen, E., Akinci, U., Bryne, J.C., Hou, J., Gontan, C., Moen, M., Szumska, D., Kockx, C., van Ijcken, W., Dekkers, D.H., et al. (2011). Sox2 cooperates with Chd7 to regulate genes that are mutated in human syndromes. Nat. Genet. *43*, 607–611.

Fontenot, J.D., Gavin, M.A., and Rudensky, A.Y. (2003). Foxp3 programs the development and function of CD4+CD25+ regulatory T cells. Nat. Immunol. *4*, 330–336.

Gattinoni, L., Zhong, X.S., Palmer, D.C., Ji, Y., Hinrichs, C.S., Yu, Z., Wrzesinski, C., Boni, A., Cassard, L., Garvin, L.M., et al. (2009). Wnt signaling arrests effector T cell differentiation and generates CD8+ memory stem cells. Nat. Med. *15*, 808–813.

Gavin, M.A., Rasmussen, J.P., Fontenot, J.D., Vasta, V., Manganiello, V.C., Beavo, J.A., and Rudensky, A.Y. (2007). Foxp3-dependent programme of regulatory T-cell differentiation. Nature *445*, 771–775.

Glant, T.T., and Mikecz, K. (2004). Proteoglycan aggrecan-induced arthritis: a murine autoimmune model of rheumatoid arthritis. Methods Mol. Med. *102*, 313–338.

Guo, Z., Dose, M., Kovalovsky, D., Chang, R., O'Neil, J., Look, A.T., von Boehmer, H., Khazaie, K., and Gounari, F. (2007). Beta-catenin stabilization stalls the transition from double-positive to single-positive stage and predisposes thymocytes to malignant transformation. Blood *109*, 5463–5472.

Han, G.M., Zhao, B., Jeyaseelan, S., and Feng, J.M. (2009). Age-associated parallel increase of Foxp3(+)CD4(+) regulatory and CD44(+)CD4(+) memory T cells in SJL/J mice. Cell. Immunol. *258*, 188–196.

Hassman, R.A., Lazarus, J.H., Dieguez, C., Weetman, A.P., Hall, R., and McGregor, A.M. (1985). The influence of lithium chloride on experimental autoimmune thyroid disease. Clin. Exp. Immunol. *61*, 49–57.

Hori, S., Nomura, T., and Sakaguchi, S. (2003). Control of regulatory T cell development by the transcription factor Foxp3. Science *299*, 1057–1061.

Khattri, R., Cox, T., Yasayko, S.A., and Ramsdell, F. (2003). An essential role for Scurfin in CD4+CD25+ T regulatory cells. Nat. Immunol. *4*, 337–342.

Lai, J.S., and Herr, W. (1992). Ethidium bromide provides a simple tool for identifying genuine DNA-independent protein associations. Proc. Natl. Acad. Sci. USA *89*, 6958–6962.

Lindley, S., Dayan, C.M., Bishop, A., Roep, B.O., Peakman, M., and Tree, T.I. (2005). Defective suppressor function in CD4(+)CD25(+) T-cells from patients with type 1 diabetes. Diabetes *54*, 92–99.

Manicassamy, S., Reizis, B., Ravindran, R., Nakaya, H., Salazar-Gonzalez, R.M., Wang, Y.C., and Pulendran, B. (2010). Activation of beta-catenin in dendritic cells regulates immunity versus tolerance in the intestine. Science *329*, 849–853.

Marson, A., Kretschmer, K., Frampton, G.M., Jacobsen, E.S., Polansky, J.K., MacIsaac, K.D., Levine, S.S., Fraenkel, E., von Boehmer, H., and Young, R.A. (2007). Foxp3 occupancy and regulation of key target genes during T-cell stimulation. Nature *445*, 931–935.

Mempel, T.R., Pittet, M.J., Khazaie, K., Weninger, W., Weissleder, R., von Boehmer, H., and von Andrian, U.H. (2006). Regulatory T cells reversibly suppress cytotoxic T cell function independent of effector differentiation. Immunity *25*, 129–141.

Mottet, C., Uhlig, H.H., and Powrie, F. (2003). Cutting edge: cure of colitis by CD4+CD25+ regulatory T cells. J. Immunol. *170*, 3939–3943.

Ono, M., Yaguchi, H., Ohkura, N., Kitabayashi, I., Nagamura, Y., Nomura, T., Miyachi, Y., Tsukada, T., and Sakaguchi, S. (2007). Foxp3 controls regulatory T-cell function by interacting with AML1/Runx1. Nature *446*, 685–689.

Reya, T., Duncan, A.W., Ailles, L., Domen, J., Scherer, D.C., Willert, K., Hintz, L., Nusse, R., and Weissman, I.L. (2003). A role for Wnt signalling in self-renewal of haematopoietic stem cells. Nature *423*, 409–414.

Roord, S.T., de Jager, W., Boon, L., Wulffraat, N., Martens, A., Prakken, B., and van Wijk, F. (2008). Autologous bone marrow transplantation in autoimmune arthritis restores immune homeostasis through CD4+CD25+Foxp3+ regulatory T cells. Blood *111*, 5233–5241.

Samstein, R.M., Arvey, A., Josefowicz, S.Z., Peng, X., Reynolds, A., Sandstrom, R., Neph, S., Sabo, P., Kim, J.M., Liao, W., et al. (2012). Foxp3 exploits a pre-existent enhancer landscape for regulatory T cell lineage specification. Cell *151*, 153–166.

Sarantidis, D., and Waters, B. (1983). A review and controlled study of cutaneous conditions associated with lithium carbonate. Br. J. Psychiatry *143*, 42–50.

Sato, N., Meijer, L., Skaltsounis, L., Greengard, P., and Brivanlou, A.H. (2004). Maintenance of pluripotency in human and mouse embryonic stem cells through activation of Wnt signaling by a pharmacological GSK-3-specific inhibitor. Nat. Med. *10*, 55–63.

Staal, F.J., Luis, T.C., and Tiemessen, M.M. (2008). WNT signalling in the immune system: WNT is spreading its wings. Nat. Rev. Immunol. *8*, 581–593.

Stern, J.B., and Smith, K.A. (1986). Interleukin-2 induction of T-cell G1 progression and c-myb expression. Science *233*, 203–206.

Thompson, C.J., and Baylis, P.H. (1986). Asymptomatic Graves' disease during lithium therapy. Postgrad. Med. J. *62*, 295–296.

Tiemessen, M.M., Baert, M.R., Schonewille, T., Brugman, M.H., Famili, F., Salvatori, D.C., Meijerink, J.P., Ozbek, U., Clevers, H., van Dongen, J.J., and Staal, F.J. (2012). The nuclear effector of Wnt-signaling, Tcf1, functions as a T-cell-specific tumor suppressor for development of lymphomas. PLoS Biol. *10*, e1001430.

van Loosdregt, J., Vercoulen, Y., Guichelaar, T., Gent, Y.Y., Beekman, J.M., van Beekum, O., Brenkman, A.B., Hijnen, D.J., Mutis, T., Kalkhoven, E., et al. (2010). Regulation of Treg functionality by acetylation-mediated Foxp3 protein stabilization. Blood *115*, 965–974.

van Loosdregt, J., Brunen, D., Fleskens, V., Pals, C.E., Lam, E.W., and Coffer, P.J. (2011). Rapid temporal control of Foxp3 protein degradation by sirtuin-1. PLoS ONE *6*, e19047.

van Loosdregt, J., Fleskens, V., Fu, J., Brenkman, A.B., Bekker, C.P., Pals, C.E., Meerding, J., Berkers, C.R., Barbi, J., Gröne, A., et al. (2013). USP7/HAUSP-mediated stabilization of Foxp3 increases Treg suppressive capacity. Immunity *39*, this issue, 259–271.

Verbeek, S., Izon, D., Hofhuis, F., Robanus-Maandag, E., te Riele, H., van de Wetering, M., Oosterwegel, M., Wilson, A., MacDonald, H.R., and Clevers, H. (1995). An HMG-box-containing T-cell factor required for thymocyte differentiation. Nature *374*, 70–74.

Viglietta, V., Baecher-Allan, C., Weiner, H.L., and Hafler, D.A. (2004). Loss of functional suppression by CD4+CD25+ regulatory T cells in patients with multiple sclerosis. J. Exp. Med. *199*, 971–979.

Wehrens, E.J., Mijnheer, G., Duurland, C.L., Klein, M., Meerding, J., van Loosdregt, J., de Jager, W., Sawitzki, B., Coffer, P.J., Vastert, B., et al. (2011). Functional human regulatory T cells fail to control autoimmune inflammation due to PKB/c-akt hyperactivation in effector cells. Blood *118*, 3538–3548.

Wildin, R.S., Ramsdell, F., Peake, J., Faravelli, F., Casanova, J.L., Buist, N., Levy-Lahad, E., Mazzella, M., Goulet, O., Perroni, L., et al. (2001). X-linked neonatal diabetes mellitus, enteropathy and endocrinopathy syndrome is the human equivalent of mouse scurfy. Nat. Genet. *27*, 18–20.

Willert, K., Brown, J.D., Danenberg, E., Duncan, A.W., Weissman, I.L., Reya, T., Yates, J.R., 3rd, and Nusse, R. (2003). Wnt proteins are lipid-modified and can act as stem cell growth factors. Nature *423*, 448–452.

Wu, Y., Borde, M., Heissmeyer, V., Feuerer, M., Lapan, A.D., Stroud, J.C., Bates, D.L., Guo, L., Han, A., Ziegler, S.F., et al. (2006). FOXP3 controls regulatory T cell function through cooperation with NFAT. Cell *126*, 375–387.

Yan, K.X., Fang, X., Han, L., Zhang, Z.H., Kang, K.F., Zheng, Z.Z., and Huang, Q. (2010). Foxp3+ regulatory T cells and related cytokines differentially expressed in plaque vs. guttate psoriasis vulgaris. Br. J. Dermatol. *163*, 48–56.

Zaiss, D.M., van Loosdregt, J., Gorlani, A., Bekker, C.P., Gröne, A., Sibilia, M., van Bergen en Henegouwen, P.M., Roovers, R.C., Coffer, P.J., and Sijts, A.J. (2013). Amphiregulin enhances regulatory T cell-suppressive function via the epidermal growth factor receptor. Immunity *38*, 275–284.

Zhou, X., Yu, S., Zhao, D.M., Harty, J.T., Badovinac, V.P., and Xue, H.H. (2010). Differentiation and persistence of memory CD8(+) T cells depend on T cell factor 1. Immunity *33*, 229–240.